

## Hydrogenation of ZnO:Al Thin Films Using Hot Filament

Ilsein An, Ok Kyung Kim, Chang-Hyo Lee and You Shin Ahn

*Department of Physics, Hanyang University, Ansan, Korea*

*LG. Philips LCD, Kumi, Korea*

(Received June 30, 2000)

**Abstract** – ZnO : Al films were prepared through the optimization process of aluminum content and substrate temperature in rf-magnetron sputtering. When hydrogenation was performed on these films using a hot filament method, all films showed improvement in conductivity although more conductive film showed less improvement. When the substrate temperature ( $T_H$ ) was varied from 25°C to 300°C during hydrogenation, the resistivity was reduced more at higher  $T_H$  but the recovery of resistivity was observed upon the extinction of hot filament. This dehydrogenation was caused by the hydrogen evolution out of the film and it was more severe at higher  $T_H$  (more than 30% at  $T_H = 300^\circ\text{C}$ ) Thus, two methods were developed to suppress the dehydrogenation in ZnO : Al films : (1) capping with amorphous silicon thin film as a diffusion barrier, and (2) cooling during hydrogenation.

### I. Introduction

Zinc oxide (ZnO) films show several advantages when used as transparent conducting electrodes, especially for the windows of solar cells [1, 2]. The lower cost of the material compared to indium tin oxide (ITO) and its high transmission over wide spectral range and its stability in hydrogen ambient are among them [3, 4]. When ZnO is doped with foreign elements such as Ga, Al, Si, its optical gap widens through the filling of narrow conduction band and its conductivity increases [5-7]. However, more efforts are needed to achieve a conductivity comparable to that of commonly used ITO [8-10].

Besides those elements, hydrogen is also known to widen the band gap and increase the conductivity of ZnO through the removal of oxygen vacancies [11-13]. Secondary ion mass spectrometer (SIMS) and real-time spectroscopic ellipsometry studies revealed that hydrogen could easily penetrate a few hundred angstroms into ZnO film when atomic hydrogens were generated from a hot filament source [14, 15]. Thus, hydrogen can be used as doping element which can be inserted after films are formed.

In this work we sputtered various aluminum doped ZnO (ZnO:Al) films by varying aluminum content and substrate temperature. Hydrogenation was performed on those films and the evolution of

resistance was measured in real-time. We found real-time measurements were important to observe the hydrogenation and dehydrogenation effects. In order to preserve high conductivity of ZnO:Al films after hydrogenation, the dehydrogenation should be suppressed. We show the results of cooling and over-layer methods which we developed for this goal.

### II. Experiment

For the deposition of high conductivity ZnO:Al films we varied deposition temperature ( $T_S$ ) and aluminum content in an rf-magnetron sputtering. Aluminum content was varied by mixing of  $\text{Al}_2\text{O}_3$  and ZnO powder during target fabrication. For the post-hydrogenation study, tungsten filament was ignited in 8 mTorr hydrogen ambient. It has been demonstrated that the hot-filament technique is a very efficient method to produce atomic hydrogen [14]. For electrical measurements glass substrate with two parallel chromium electrodes was used. For real-time measurements, ZnO : Al film was sputtered on this substrate and two electrodes were connected to the programmable electrometer via feedthrough in vacuum chamber. Although much thicker films showed better conductivity, most of the films used in this study were around 1000 Å thick for better hydrogen diffusion.

### III. Results and Discussion

When we varied deposition conditions, the most conductive ZnO : Al film was obtained at substrate temperature of  $>200^{\circ}\text{C}$  from the target with  $\text{Al}_2\text{O}_3$  content ( $C_{\text{Al}}$ ) of 2.0-2.2 wt.% in our system. The actual aluminum content in ZnO : Al films were close to that of targets. Fig. 1 shows the resistivities of ZnO : Al films as function of  $C_{\text{Al}}$  (top) and  $T_{\text{S}}$  (bottom). The trend in the top of Fig. 1 is well known [7]. These films were exposed to atomic hydrogen at different hydrogenation temperature ( $T_{\text{H}}$ ) and resistances were measured in real-time. When the signals approached asymptotic values, we assumed that ZnO : Al films were almost soaked in atomic hydrogen based on earlier studies [14]. Typical data will be seen later in Fig. 6. Fig. 2 shows the post-hydrogenation effects on ZnO : Al films with different aluminum content. From the Arrhenius plots using the  $T_{\text{H}}$ -dependent resistances, we found quite linear behaviors below  $200^{\circ}\text{C}$  in all samples (top). The bottom panel shows the activation energies

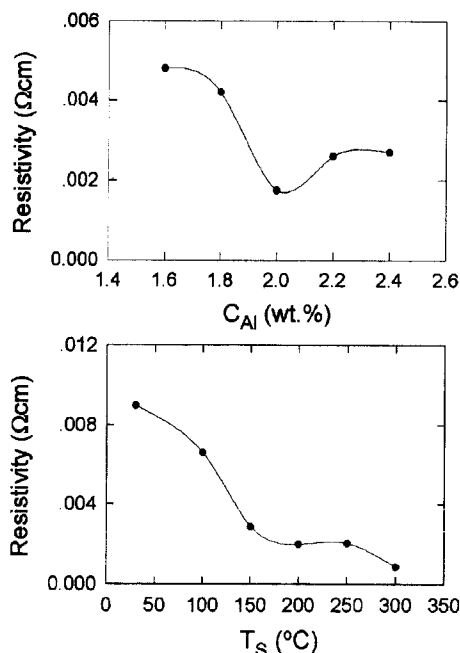


**Fig. 1.** Top: The resistivity of ZnO : Al films as a function of the wt.% of  $\text{Al}_2\text{O}_3$  in target used ( $T_{\text{S}}$  was kept at  $250^{\circ}\text{C}$ ). Bottom: The resistivity of ZnO : Al films as a function of the deposition temperature,  $T_{\text{S}}$ . (target with 2.0 wt.% of  $\text{Al}_2\text{O}_3$  was used).

for the hydrogenation process in different samples (filled circles), which were deduced from the slopes of the Arrhenius plots in the upper panel. Fig. 3 depicts similar results for the ZnO : Al films grown at different  $T_{\text{S}}$ .

The pure temperature-dependence of resistivity in semiconducting ZnO : Al is negligible as we can see in Fig. 4. In the bottom panels of both Fig. 2 and Fig. 3, open circles denote the data obtained during dehydrogenation process by turning off hot filament while keeping constant  $T_{\text{H}}$  and hydrogen flow. We notice that the variation of the activation energy over deposition parameters (bottom figures in Fig. 2 and Fig. 3) resembles that of the resistivity of the as-grown film (Fig. 1). That is, poorly conductive ZnO:Al film can be improved more if we use post-hydrogenation technique.

Fig. 5 shows the resistivities of the samples shown in Fig. 1 before (filled circles) and after 100 s of post-hydrogenation at  $T_{\text{H}} = 300^{\circ}\text{C}$  (open circles).

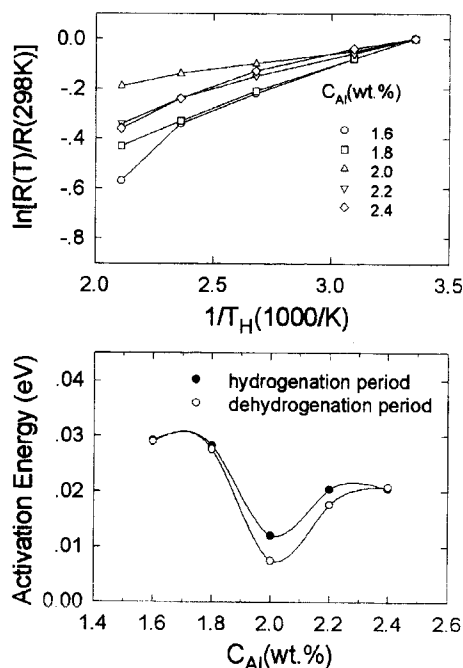


**Fig. 2.** Top: The Arrhenius plot of the resistance obtained from the post-hydrogenation of ZnO : Al films sputtered from targets with different  $\text{Al}_2\text{O}_3$  content. Resistances from were normalized by that of room temperature. Bottom: Activation energy for the hydrogenation process. Filled circles were obtained during hydrogenation and open circles were obtained during dehydrogenation process.

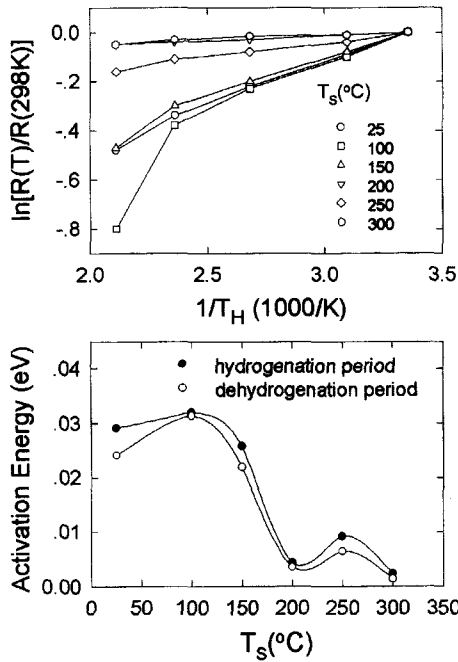


**Fig. 3.** Top: The Arrhenius plot of the resistance obtained from the hydrogenation of ZnO : Al films prepared at different  $T_S$ . Resistances were normalized by that of room temperature. Bottom: Activation energy for the hydrogenation process. Filled circles were obtained during hydrogenation and open circles were obtained during dehydrogenation process.

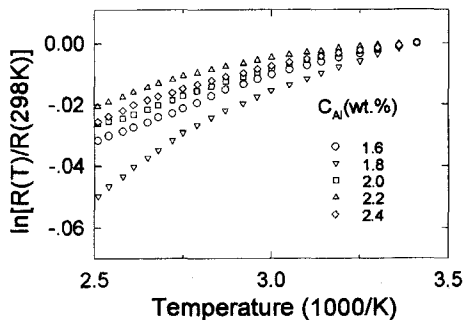


**Fig. 4.** The temperature dependence of the resistivity of semiconducting ZnO : Al films. The magnitude is small compared to those in Figs. 3 and 4.

Although ZnO : Al prepared at  $C_{Al} = 2.0$  wt.% still shows the lowest resistivity, the variation over samples becomes much smaller and overall values lie between 0.001 and 0.002  $\Omega\cdot\text{cm}$ . This indicates that when we varied deposition parameters,  $T_S$  or  $C_{AlO}$ , the generation of oxygen vacancies was an important

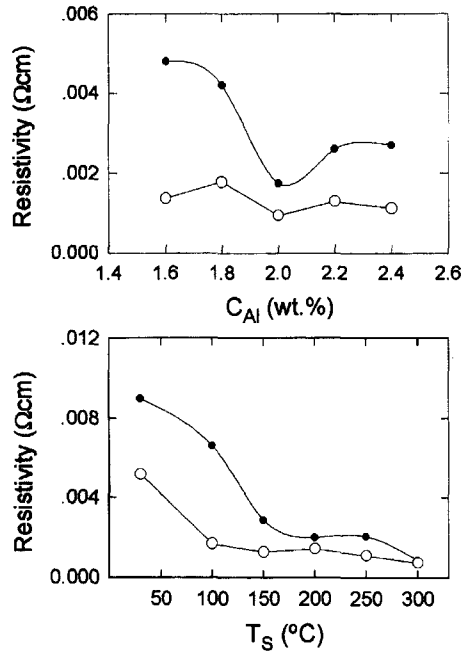


**Fig. 5.** The reduction of resistivity in ZnO : Al films shown in Fig. 1 after 100 s of hydrogenation at  $T_H = 300^\circ\text{C}$ . Filled circles and open circles denote the resistivity of ZnO : Al films before and after hydrogenation, respectively.

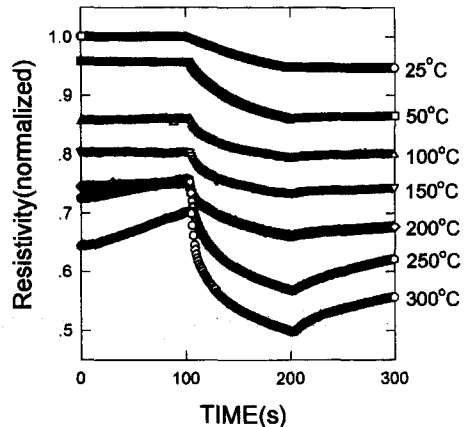


**Fig. 6.** The normalized resistance measured during the hydrogenation and dehydrogenation of ZnO : Al. (The sample used for this study was the one prepared at  $T_S = 250$  and  $C_{Al} = 2.0$  wt.%) Hydrogenation temperatures were  $25^\circ\text{C}$ ,  $50^\circ\text{C}$ ,  $100^\circ\text{C}$ ,  $150^\circ\text{C}$ ,  $200^\circ\text{C}$ ,  $250^\circ\text{C}$ , and  $300^\circ\text{C}$  from the top. Each hydrogenation temperature was set for a few minutes after the end of dehydrogenation ( $t = 300$  s) and the filament was ignited at  $t = 100$  s and extinguished at  $t = 200$  s).

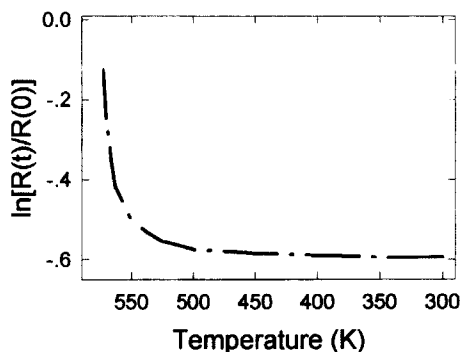


**Fig. 7.** The normalized resistance measured during hydrogenation. But the heater for the substrate was turned off so that  $T_H$  can vary from  $300^\circ\text{C}$  to room temperature. The data near room temperature were measured over many hours after termination of hydrogenation (The sample used for this study was the one prepared at  $T_S = 250$  and  $C_{Al} = 2.0$  wt.%).

factor to determine the electrical conductivity of ZnO:Al film. Thus, post-hydrogenation generated more oxygen vacancies from less conductive films.

However, as we already mentioned, there was dehydrogenation effect when we extinguished filament. Fig. 6 shows the evolution of resistivity during hydrogenation and dehydrogenation processes at various  $T_H$  in one of the ZnO:Al film. Filament was turned on at time  $t = 100$  s and turned off at  $t = 200$  s. It is evident from the figure that hydrogenation is more effective at an elevated temperature but dehydrogenation also becomes more active. Apparently hydrogen evolves out right after the extinction of filament. We devised two techniques in order to prevent the out-diffusion of hydrogen after the termination of hydrogenation.

The first method is lowering  $T_H$  (cooling substrate temperature) while keeping the hydrogenation process. Fig. 7 shows the effect of cooling down from the initial hydrogenation of  $T_H = 300^\circ\text{C}$  to room temperature. Cooling took place over several hours and measurements were continued for many hours after  $T_H$  reached room temperature and finally the filament was turned off. The success of the cooling method was already seen in Fig. 6, where dehydrogenation at room temperature was negligible. This sample held improved conductivity very well after termination of hydrogenation and could be used later

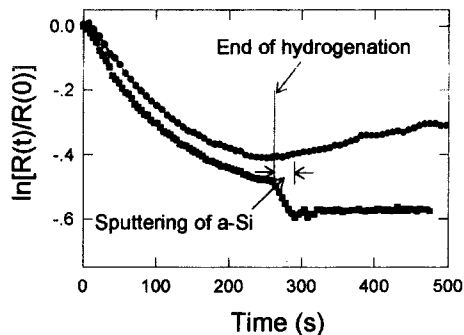


**Fig. 8.** The normalized resistance measured during and after termination of hydrogenation (filled circles). Same experiment but  $\sim 30 \text{ \AA}$  of a-Si deposition was followed by right after termination of hydrogenation (filled squares) (The sample used for this study was the one prepared at  $T_S = 250$  and  $C_{Al} = 2.0$  wt.%).

for room temperature applications. The other method is to deposit overlayer to prevent the out-diffusion through ZnO:Al surface. Fig. 8 shows the hydrogenation process at  $T_H = 250^\circ\text{C}$  followed by the deposition of  $\sim 30 \text{ \AA}$  of amorphous silicon (a-Si) layer (filled squares). The slight decrease in resistance right after the deposition of a-Si might be caused by the doping of silicon through the ZnO:Al surface and doped a-Si layer. Compared to the normal termination of hydrogenation which shows dehydrogenation effect (filled circles), a-Si covered ZnO:Al shows stable low resistivity (filled squares). This method can be useful for solar cell application. In p-i-n solar cell structure, p-type amorphous silicon can be deposited on ZnO:Al right after post-hydrogenation.

#### IV. Conclusion

We showed the post-hydrogenation effect on variously prepared ZnO:Al films using hot filament method. The activation energy for the process was determined from the temperature dependence of resistivity showing more enhanced conductivity in less conductive film. However, the out-diffusion of hydrogen after extinction of filament caused recovery of resistivity of the films. We developed two different methods to suppress the out-diffusion of hydrogen so that we can preserve the high conductivity of ZnO:Al films after termination of hydrogenation.

### Acknowledgment

This work was supported by the Korea Research Foundation through Brain Korea 21 project.

### References

- [1] W. W. Wenas, A. Yamada, K. Takahashi, M. Yoshino, and M. Konagai, *J. Appl. Phys.* **70**, 7119 (1991).
- [2] M. Yoshino, W. W. Wenas, A. Yamada, M. Konagai, and K. Takahashi, *Jpn. J. Appl. Phys.* **32**, 726 (1993).
- [3] M. Kitagawa, K. Mori, S. Ishihara, M. Ohno, T. Hirao, Y. Yoshioka, and S. Kohiki, *J. Appl. Phys.* **54**, 3269 (1983).
- [4] S. Major, S. Kumar, M. Bhatnagar, and K. Chopra, *Appl. Phys. Lett.* **49**, 394 (1986).
- [5] B. E. Semelius, K.-F. Berggren, J.-C. Jin, I. Hamberg, and C. G. Granqvist, *Phys. Rev. B* **37**, 10244 (1988).
- [6] G. A. Hirata, J. McKittrick, J. Siqueiros, O. A. Lopez, T. Cheeks, O. Contreras, and J. Y. Yi, *J. Vac. Sci. Technol. A* **14**, 791 (1996).
- [7] Z.-C. Jin, I. Hamberg, and C. G. Granqvist, *J. Appl. Phys.* **64**, 5117 (1988).
- [8] T. Minami, H. Nanto, and S. Takata, *Thin Solid Films*, **124**, 43 (1985).
- [9] Y. Igasaki and H. Saito, *J. Appl. Phys.* **69**, 2190 (1985).
- [10] K. Tominaga, H. Manabe, N. Umezu, I. Mori, T. Ushiro, and I. Nakabayashi, *J. Vac. Sci. Technol. A* **15**, 1074 (1997).
- [11] E. Burstein, *Phys. Rev.* **93**, 632 (1954); T. S. Moss, *Proc. Phys. Soc. London, Ser. B* **67**, 775 (1954).
- [12] T. Minami, H. Nanto, S. Shooji, and S. Takata, *Thin Solid Films*, **111**, 167 (1984).
- [13] S. Sarkar, S. Ghosh, S. Chaudhuri, and A. K. Pal, *Thin Solid Films*, **204**, 255 (1991).
- [14] Ilsin An, Y. Li, C. R. Wronski, and R. W. Collins, *Phys. Rev. B* **48**, 4464 (1993).
- [15] I. An, Y. Lu, C. R. Wronski, and R. W. Collins, *Appl. Phys. Lett.* **64**, 3317 (1994).